

Research Paper

Thermomechanical Comparison Between Bobbin and Conventional Friction Stir Welding of A356 Aluminum Alloy

Mostafa Akbari*, Milad Esfandiar, Hossein Rahimi Asiabaraki, Yaghuob Dadgar Asl, Ezatollah Hassanzadeh

Department of Mechanical Engineering, Technical and Vocational University (TVU), Tehran, Iran

ARTICLE INFO

Article history:

Received 5 December 2023
Accepted 19 February 2024
Available online 1 May 2023

Keywords:

FSW
BTFSW
Force
Strain
Temperature.

ABSTRACT

Friction Stir Welding (FSW) is a welding technique that has brought significant advancements to the field of metal joining. An innovative variation of this technique is known as bobbin tool friction stir welding (BTFSW). This study aimed to compare various aspects, including force, temperature, and strain, between FSW and BTFSW. For this reason, the finite element method was employed, utilizing the Eulerian technique to model the welding process. The findings revealed that the presence of two shoulders in BTFSW enhances heat generation by increasing the contact area with the workpiece, resulting in improved frictional heat production. The advancing side of the BFSW sample exhibited the highest recorded peak temperature, reaching 532°C. On the other hand, the CFSW sample displayed a comparatively lower peak temperature of approximately 347°C. The elevated temperature in BTFSW enhances material flowability and plasticity, leading to reduced longitudinal forces compared to FSW. In CFSW, the longitudinal force varies between 3500 N and 2500 N, whereas in BTFSW, the longitudinal force is significantly lower, approximately 800 N. Furthermore, analysis of strain distribution demonstrated that BTFSW exhibits an hourglass-shaped strain pattern, indicating a larger area affected by strain when compared to FSW. These results highlight the benefits of BTFSW in terms of enhanced heat generation, reduced forces, and a larger strain-affected area, underscoring its potential as a superior welding technique.

Citation: Akbari, M. ; Esfandiar, M.; Rahimi Asiabaraki, H.; Dadgar Asl, Y.; Hassanzadeh, E. (2023). Thermomechanical Comparison Between Bobbin and Conventional Friction Stir Welding of A356 Aluminum Alloy, Journal of Advanced Materials and Processing, 11 (2), 65-75. Doi: 10.71670/jmatpro.2024.981641

Copyrights:

Copyright for this article is retained by the author (s), with publication rights granted to Journal of Advanced Materials and Processing. This is an open – access article distributed under the terms of the Creative Commons Attribution License (<http://creativecommons.org/licenses/by/4.0>), which permits unrestricted use, distribution and reproduction in any medium, provided the original work is properly cited.



* **Corresponding Author:**

E-Mail: mr.mostafaakbari@yahoo.com

1. Introduction

Friction Stir Welding (FSW) is a cutting-edge welding technique that has revolutionized the field of metal joining [1, 2]. Unlike conventional welding methods involving melting and solidification, FSW creates high-quality, defect-free welds using frictional heat generated by a rotating tool [3, 4]. This tool, with a specially designed pin and shoulder, plunges into the adjoining metal surfaces, generating heat and mechanical agitation. As the tool moves along the joint, it stirs and forges the metal, creating a solid-state bond without reaching the melting point [5]. This unique process results in numerous advantages, including superior joint strength, enhanced mechanical properties, and improved weld quality. FSW is highly versatile and can be applied to various metals, including aluminum [6, 7], steel [8, 9], and titanium [10-12], making it an invaluable technology across industries like aerospace, automotive, and shipbuilding [13]. With its ability to produce strong, reliable, and lightweight welded structures, FSW has emerged as a game-changing solution for achieving efficient and durable metal joints [14].

Bobbin tool friction stir welding (BTFSW) is an innovative variation of the conventional friction stir welding technique [15]. Also known as self-support FSW or self-reacting FSW, this unique process has several advantages that make it a compelling choice for joining different metals, including aluminum [16-18], magnesium [19], and copper [20]. One notable distinction of BTFSW is the incorporation of an additional shoulder, referred to as the lower shoulder, at the pin end [21]. This modification enhances the welding process and offers improved weld quality compared to traditional FSW methods. Esmaily et al. [22] conducted a comparison between conventional friction stir welding and bobbin tool friction stir welding techniques. Firstly, they found that the BTFSW joints exhibited a significantly finer grain structure compared to the conventional FSW joints. Secondly, the BTFSW joints displayed higher hardness values when compared to the conventional FSW joints. This increase in hardness indicates enhanced mechanical properties in the BTFSW joints. Fuse et al. [23] examined the microstructure and mechanical properties of joining dissimilar alloys of Al/Cu using two different techniques of CFSW and BTFSW. The results indicated that the weld joints created with BTFSW exhibited higher strength compared to those produced with CFSW. Furthermore, the maximum hardness values were reported as 214 HV for BTFSW and 211 HV for CFSW, both measured at the stir zone.

Despite the considerable attention that the BTFSW method has garnered from researchers and application engineers, its application in production remains relatively rare [21]. This can be attributed, in part, to the limited availability of comprehensive studies that thoroughly investigate the disparities in thermal history, strain, and properties between weldments produced using conventional FSW and BTFSW [15, 24]. While FSW has been extensively studied and implemented in various industries, BTFSW presents unique characteristics and advantages that have yet to be fully explored and understood. A more thorough understanding of the thermal behavior, strain distribution, and resulting material properties in BTFSW weldments is crucial for engineers and manufacturers to integrate this technique into their production processes confidently.

2. Simulation details

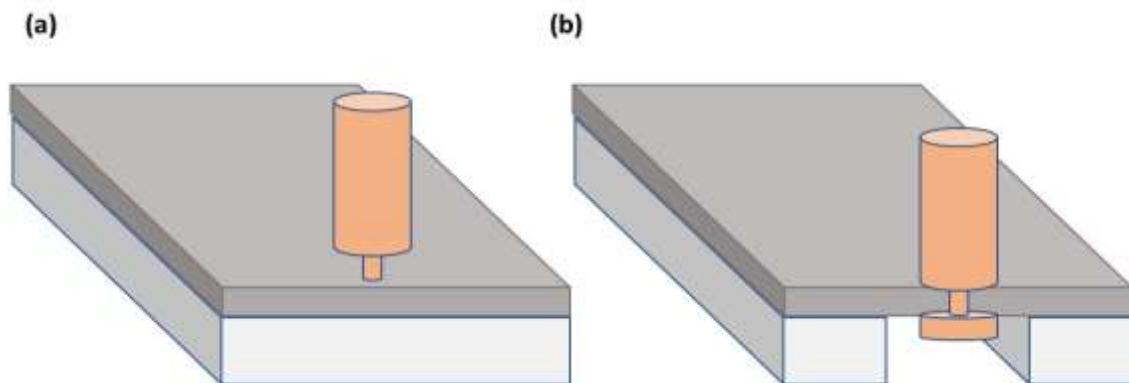
To comprehensively investigate the temperature distribution, strain patterns, and force during the FSW and BTFSW, the Deform-3D™ software was utilized as a powerful simulation tool. In this particular study, a 3-D Lagrangian incremental finite element method was chosen as the numerical simulation approach for accurately modeling the process dynamics. Several assumptions were made to simplify the problem. These assumptions are outlined below:

1. The material model was considered to be rigid-visco-plastic.
2. Both the tool and the backing plate were assumed to be rigid. This assumption disregards any deformations or flexibility in the tool and backing plate during the process.
3. The friction factor between the tool and the workpiece was assumed to be constant throughout the process.
4. The thermal properties of both the workpiece and the tool were assumed to be constant.
5. The free surfaces of both the workpiece and the tool were assumed to experience free convection at an ambient temperature of 20 °C.

In this study, traverse and tool rotational speeds of 60 mm/min and 900 rpm were used to produce all joints. Friction stir welding and bobbin tool friction stir welding methods were employed to join aluminum profiles in a butt configuration, as illustrated in Figure 1. The FSW was performed on A356 aluminum with a thickness of 6 mm, and the chemical compositions are given in Table 1.

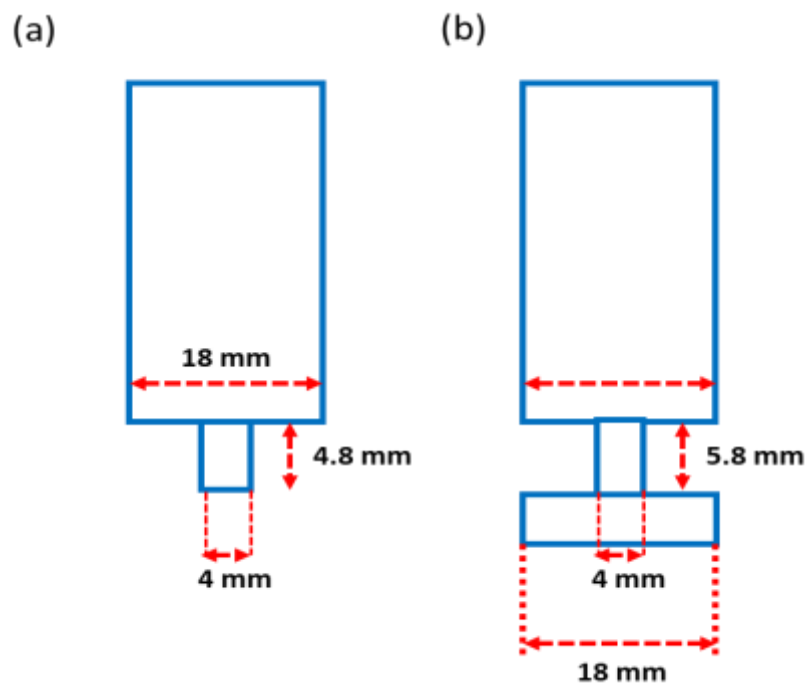
Table 1. Chemical composition of as-cast A356 aluminum plates (wt%).

Si	Fe	Mn	Cu	Zn	Ti	Mg
7	0.31	0.1	0.2	0.1	0.25	0.3

**Fig. 1.** Schematic representation of a) FSW, b) BTFSW

For the FSW process, a specialized tool configuration was utilized. The FSW tool consisted of a shoulder with a diameter of 18 mm. Additionally, it incorporated a cylindrical pin design with a diameter of 4 mm (Figure 2). In the case of the BTFSW technique, a fixed gap bobbin tool was employed. This

tool configuration included both an upper and a lower shoulder with a diameter of 18 mm. The pin diameter is 4 mm. The fixed gap between the shoulders was maintained at 5.8 mm. The BTFSW method offers distinct advantages due to its specialized tool design and operational principles [25].

**Fig. 2.** Dimensions of a) FSW, b) BTFSW tools

The tool employed in the simulation was treated as a rigid body and discretized with tetrahedral elements to capture its intricate behavior. In addition, to accurately represent the workpiece and its response to the FSW tool, the workpiece was divided into

multiple zones and meshed using different element sizes. Specifically, smaller elements with a mean length of 0.8 mm were concentrated in the vicinity of the FSW tool to improve the simulation accuracy, as depicted in Figure 3.

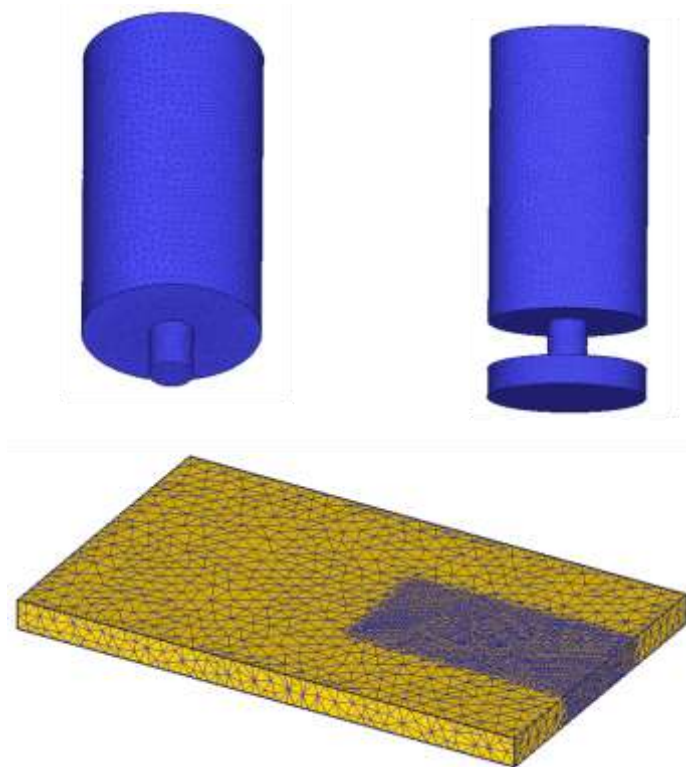


Fig. 3. Illustration of the workpiece and the FSW tools.

The flow stress of A356 aluminum alloy is given as a function of strain rate, plastic strain, and temperature [26, 27]:

$$\bar{\sigma} = \bar{\sigma}(\bar{\epsilon}, \dot{\bar{\epsilon}}, T) \tag{1}$$

where $\bar{\sigma}$ represents the flow stress, $\bar{\epsilon}$ represents the plastic strain, $\dot{\bar{\epsilon}}$ represents the strain rate, and T is the temperature.

Constant shear friction is utilized to model friction between the tool and workpiece, mainly in this study. In the constant shear model, the frictional force could be calculated as follows [27]:

$$f = mk \tag{2}$$

where f , k , and m represent the frictional stress at the tool-workpiece interface, the shear yield stress, and the shear friction factor, respectively.

Moreover, the convective boundary condition for all weldment surfaces is defined as:

$$k \frac{\partial T}{\partial n} = h(T - T_{amb}) \tag{3}$$

where h represents the convection coefficient, T_{amb} is the ambient temperature, and n is the boundary's normal vector. The coefficient of convection for the sample's surfaces displayed to the environment is considered 20 W/(m².°C). Moreover, the thermal properties of the H13 steel tool and A356 samples are summarized in Table 2.

Table 2. Thermal properties of the A356 aluminum alloy and H13 FSW tool

Property	A356	FSW Tool
Heat capacity (N/mm2°C)	2.57	4.5
Conductivity (W/m°C)	117	24.5
Heat transfer coefficient between tool and billet (N/°C s mm2)	11	11
Heat transfer coefficient between backing plate and billet (N/ C s mm)	5	

3. Result and discussion

3.1. Temperature comparison between FSW and BTFSW

The temperature history experienced during the FSW/BTFSW plays a crucial role in determining the material's resulting microstructure and subsequent mechanical properties. During FSW/BTFSW, the

microstructure modification of the material occurs primarily due to the intense frictional heating generated between the rotating tool and the workpiece. This frictional heating leads to localized plastic deformation and mixing of the material, resulting in the formation of a thermo-mechanically

affected zone (TMAZ) and a more extensively modified region known as the stir zone (SZ).

To achieve a fine microstructure in the SZ, generating sufficient frictional heat during the FSW process, which keeps the material in a well-plasticized state at an appropriate temperature, is crucial. This plasticized state allows for the adequate mixing and redistribution of the material, facilitating grain refinement and homogenization within the SZ.

The heat generation in FSW/BTFSW primarily occurs due to the frictional interaction between the rotating tool and the workpiece, accompanied by the plastic deformation around the tool [28, 29]. Significant heat is generated as the tool traverses through the workpiece, leading to localized softening and material flow. This heat, in combination with the mechanical action of the rotating tool, facilitates the formation of a desirable microstructure with refined grain size and improved mechanical properties.

Temperature variations were examined to analyze the disparities in temperature between the BTFSW and conventional FSW processes using numerical methods (Figure 4). It was observed that the BTFSW samples exhibited a higher peak temperature compared to the FSW sample. The results of the FSW and BTFSW samples showed that the highest recorded peak temperature (~ 532 °C) was observed in the BTFSW sample. In contrast, the CFSW sample

displayed a lower peak temperature, approximately ~ 347 °C. The shoulder component of the tool plays a crucial role in generating heat during the FSW process. In the case of the BTFSW technique, the utilization of two shoulders amplifies the heat generation within the material, surpassing that of conventional FSW. This result is consistent with previously reported results. Esmaily et al. [30] investigated the disparities in transient temperature between the BFSW and CFSW processes. They employed thermal profiles to analyze the temperature variations. The findings revealed that the BFSW samples exhibited a higher peak temperature compared to the FSW samples. The presence of two shoulders in the BTFSW tool configuration allows for an increased contact area with the workpiece. As a result, a larger amount of frictional heat is produced during the welding process. The additional heat generated by the dual shoulders enhances the plasticization and softening of the material, promoting effective mixing and material flow.

Compared to FSW, the higher heat input achieved in BTFSW can be attributed to the intensified frictional interaction between the tool and the workpiece. This elevated heat generation facilitates more significant temperature rises within the material, enhancing material deformation and mixing.

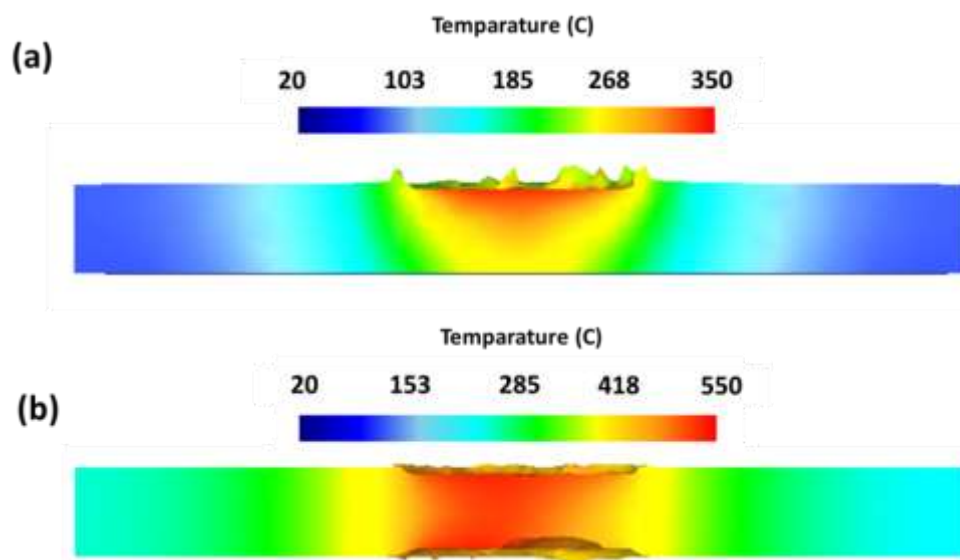


Fig. 4. Temperature variation of the sample produced by a) FSW b) BTFSW

Introducing a lower shoulder in the BTFSW technique brings about notable changes in the peak temperature and heat generation during welding. Including the lower shoulder in the BTFSW configuration provides a more balanced heat input from both sides of the plate being welded. This balanced heat distribution contributes to developing

a symmetrical microstructure on both sides of the joint.

Figure 5 illustrates the temperature variations at two different levels within the cross-sections of samples produced by both friction stir welding (FSW) and bobbin tool friction stir welding (BTFSW). The upper surface, where the temperature changes are

indicated, is located 2 mm below the workpiece surface, while the lower surface, also marked for temperature changes, is positioned 2 mm above the bottom surface of the samples.

In the case of conventional FSW, the maximum temperature recorded on the upper surface is approximately 320 degrees Celsius, which differs by 40 degrees Celsius from the temperature on the lower surface, which reaches 280 degrees Celsius. Conversely, in BTFSW, the temperature on both the upper and lower surfaces is nearly identical. This temperature homogeneity can be attributed to the presence of the lower shoulder of the tool in BTFSW. By incorporating a lower shoulder, BTFSW offers

advantages such as enhanced heat input control, improved material flow, and symmetrical microstructure formation [31]. These features make BTFSW a promising option for achieving high-quality welds with tailored material properties. Also, the maximum temperature in BTFSW can be seen in the retreating zone, which is consistent with previous studies. Li et al. [32] conducted temperature measurements using thermocouples within a 6-mm-thick 6082 aluminum alloy plate during BTFSW. Their findings revealed that the temperature on the retreating side (RS) of the weld was higher than that on the advancing side (AS).

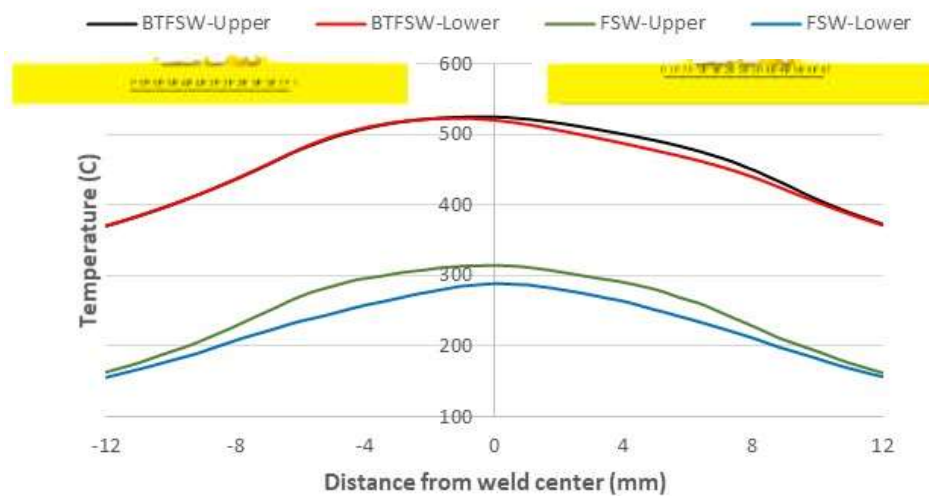


Fig. 5. Temperature profile at the different locations of the samples produced by a) FSW b) BTFSW

3.2. Force comparison between FSW and BTFSW

The force exerted on the tool during the processing is a critical factor that directly influences its wear characteristics and overall lifespan. Throughout the FSW/BTFSW process, the tool encounters various forces, including lateral, longitudinal, and axial forces [33-35].

As the FSW/BTFSW tool penetrates the specimen, an axial force is applied, creating an upward-lifting effect on the tool. This axial force results from the resistance the tool encounters as it interacts with the workpiece material. Several factors, such as material properties, process parameters, and tool design, influence the magnitude of this force [36-38].

In certain FSW/BTFSW machines, the axial force is actively controlled to maintain a consistent level throughout the process. This control ensures steady tool penetration and minimizes variations in force. On the other hand, in some FSW setups, the process is performed by controlling the tool's vertical position, which inadvertently leads to changes in the applied force during the course of the process. The

variations in force during the FSW process can have implications for the tool's performance and wear characteristics. Fluctuating forces may affect the tool's stability, leading to uneven wear patterns or increased wear rates in specific regions. Furthermore, changes in force can impact the material flow, heat generation, and resulting microstructure of the workpiece material.

Figure 6 illustrates the axial force profiles of friction stir welding (FSW) and bobbin tool friction stir welding (BTFSW). The force variations between the two methods exhibit distinct characteristics. In FSW, as the tool pin makes contact with the workpiece's surface during the plunging stage, the axial force undergoes a significant increase. This increase can be attributed to the combined effects of material softening and work hardening. The maximum axial force is observed during the plunging phase when the shoulder fully penetrates the sample.

In BTFSW, there is a notable distinction compared to conventional FSW in terms of tool entry into the workpiece. While FSW involves a vertical tool entry, BTFSW employs a sideways entry from the side of the sheet parallel to its surface. The highest force is

typically observed in FSW when the tool penetrates the sheet. Since the tool is inserted vertically in FSW, there is a substantial vertical force exerted on the tool during this process. However, in BTFSW, where the tool enters parallel to the sheet, the vertical force applied to the tool is significantly reduced (Figure 6). Additionally, the longitudinal force experienced in FSW is considerably greater compared to BTFSW. In CFSW, the longitudinal force fluctuates between 3500 N and 2500 N, while in BTFSW, the longitudinal force shows much lower values of about 800 N. This difference can be attributed to the dissimilarities in the welding processes and the presence of the lower shoulder in BTFSW.

In BTFSW, the inclusion of the lower shoulder leads to higher heat generation during the welding process. This elevated heat generation results in an increase in the temperature of the material being welded. As the temperature rises, the material undergoes a softening

effect, reducing its resistance to the tool. Consequently, the power required for the welding process decreases. The increased heat and temperature in BTFSW contribute to the improved flowability and plasticity of the material. This enhanced malleability allows the tool to penetrate and traverse the workpiece with reduced resistance, resulting in a reduced longitudinal force compared to FSW. Wang et al. [39] employed the BTFSW technique to join 3.2 mm thick AA2198-T851 aluminum alloy. The researchers discovered that this technique resulted in the formation of a staggered structured layer and an unbalanced force distribution between the upper and lower shoulders. These factors contributed to effective material flow in the direction of weld thickness, thereby preventing the formation of void defects. This approach demonstrated an improvement over conventional BTFSW methods.

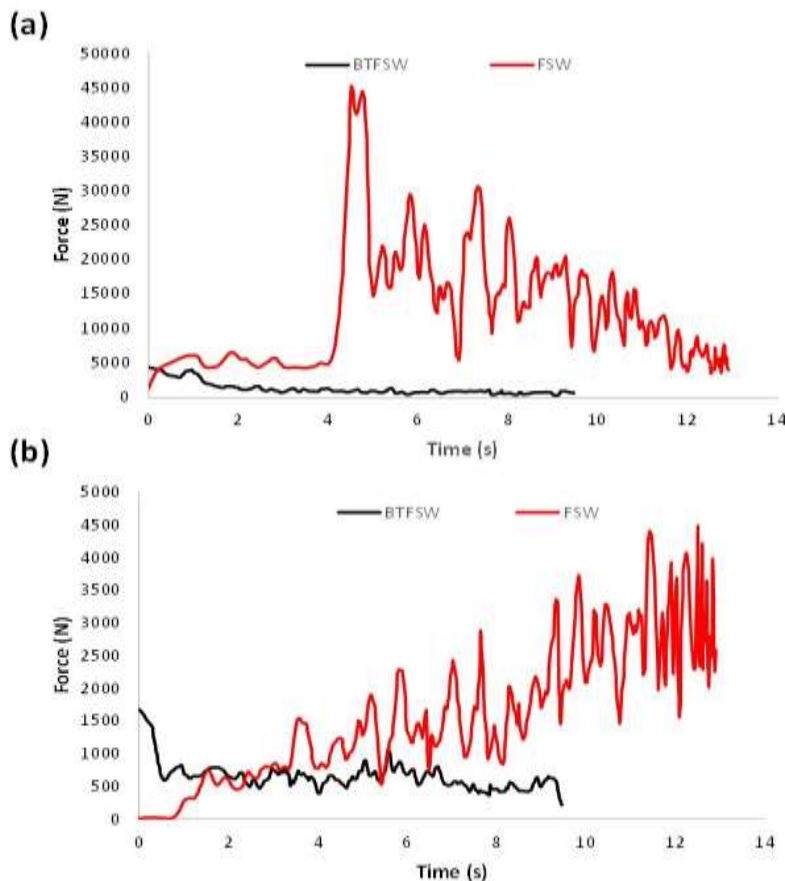


Fig. 6. Comparison of a) axial force and b) longitudinal force between FSW and BTFSW

3.3. Strain distribution in FSW and BTFSW

Strain, in the context of welding using the FSW process, refers to the localized deformation or distortion that occurs in the metal during welding. It is a physical quantity that measures the amount of deformation or change in the length of a material per unit length.

The distribution pattern of strain in FSW can be influenced by several factors, including welding parameters, tool design, material properties, and joint geometry. Excessive strain can result in defects within the welded joint, such as cracks, voids, or residual stresses. These defects can compromise the strength and durability of the joint. Therefore, it is

crucial to comprehend and control the strain distribution within acceptable limits during the FSW process optimization and quality assurance.

Figure 7 depicts the strain variations observed in the cross-sectional analysis of samples welded using both FSW and BTFSW. In FSW, the affected area exhibiting strain is typically basin-shaped, as commonly known. However, in contrast to FSW, the strain distribution in BTFSW exhibits an hourglass shape, encompassing a larger area affected by strain. Furthermore, the maximum strain experienced in BTFSW is significantly higher than that observed in FSW. This disparity can be attributed to the elevated temperature of the material during BTFSW, which is primarily influenced by the presence of the lower shoulder. The higher temperature in BTFSW induces material softening, enhancing the flowability and plasticity of the material.

Previous studies have observed an increase in strain values as the temperature rises during FSW. Akbari

et al. [40] conducted research on the impact of in-process cooling on material flow, temperature distribution, and axial force during friction stir processing (FSP) of A356 alloy. They found that the non-cooled sample exhibited higher strain values compared to the cooling-assisted samples. The researchers demonstrated that the introduction of cooling in the process resulted in a decrease in temperature, which enhanced the material's resistance against the FSW tool. This decrease in material softening led to reduced material flow and strain during the FSP process.

The distinctive strain patterns and higher strain levels in BTFSW signify the unique welding dynamics of this technique. The increased strain and improved material flow resulting from the higher temperature contribute to enhanced weld quality, improved material mixing, and desirable microstructural modifications.

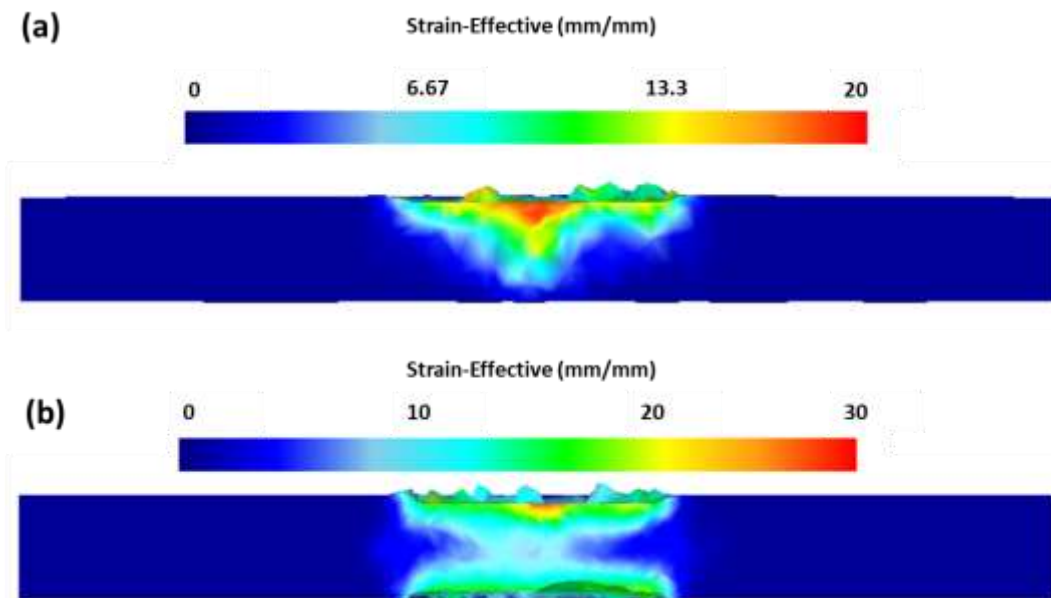


Fig. 7. Strain variation of the sample produced by a) FSW b) BTFSW

Figure 8 provides a visual representation of the cross-sectional weld morphology observed in both friction stir welding (FSW) and bobbin tool friction stir welding (BTFSW) joints. The micrographs presented for FSW showcase the AA6061-T6 alloy [41], while the micrograph for BTFSW corresponds to the AA22198-T851 alloy [42]. Notably, there are notable disparities in the cross-sectional weld morphology between the FSW and BTFSW joints.

In the case of FSW, the joint exhibits a basin-shaped morphology. This morphology is characterized by a depression or concave region in the center of the weld, resembling the shape of a basin. On the other hand, the BTFSW joint demonstrates an hourglass shape. This morphology resembles the silhouette of

an hourglass, with a narrow, constricted region at the center of the weld, expanding outward towards the edges.

The contrasting weld morphologies observed in FSW and BTFSW can be attributed to the specific material deformation patterns induced by the shoulder in each welding process. In FSW, the single shoulder exerts pressure and generates heat as it moves along the weld line. This results in localized plastic deformation and material flow, leading to the formation of the basin-shaped morphology.

In contrast, BTFSW utilizes the presence of two shoulders in its tool configuration. The additional shoulder increases the contact area with the workpiece, leading to enhanced frictional heat

generation and plasticization of the material. This increased plasticity and heat input contribute to a more extensive material mixing and deformation, resulting in the hourglass-shaped morphology observed in the BTFSW joint.

Moreover, the accuracy of a numerical prediction regarding the strain-affected area in the weld is evaluated by comparing it with experimental observations. In this case, the predicted area affected

by strain from the numerical method aligns well with the experimental observations, indicating that the numerical method correctly predicts the region in the weld where the materials undergo significant strain. This agreement between the simulation prediction and experimental findings adds to the confidence in the model's ability to accurately capture and predict the distribution of strain in the weld region.

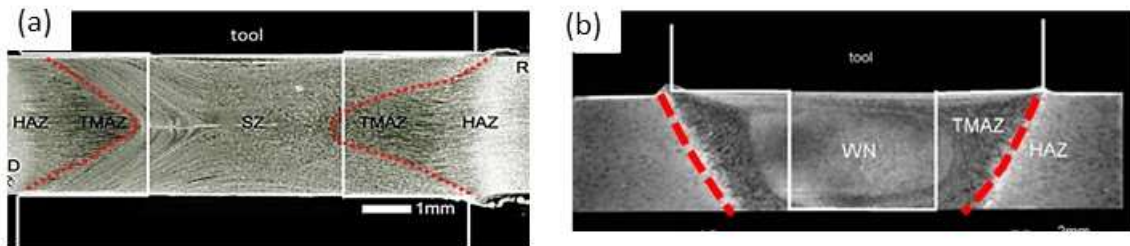


Fig. 8. Cross-sectional microstructure of joints with (a) BTFSW [42] ; and (c) CFSW [41].

4. Conclusion

The objective of this study was to conduct a comparison of multiple factors, such as force, temperature, and strain, between FSW and BTFSW. In summary, the following conclusions were achieved:

- The presence of two shoulders in the bobbin tool friction stir welding (BTFSW) configuration intensifies heat generation within the material compared to conventional friction stir welding (CFSW). This is evident from the highest recorded peak temperature of approximately 532 °C observed in the BTFSW sample. In contrast, the CFSW sample showed a lower peak temperature of around 347 °C.
- A comparison between friction stir welding (FSW) and bobbin tool friction stir welding (BTFSW) highlights significant differences in axial and longitudinal forces. BTFSW, which incorporates a lower shoulder, reduces the vertical force applied to the tool during welding. In conventional FSW, the longitudinal force varies between 3500 N and 2500 N, while in BTFSW, the longitudinal force is significantly lower, around 800 N. The increased heat and temperature in BTFSW enhance the material's flowability and plasticity, resulting in reduced longitudinal forces compared to FSW.
- Strain distribution analysis shows that BTFSW exhibits an hourglass-shaped strain distribution pattern, encompassing a larger area affected by strain compared to FSW. The higher temperature in BTFSW leads to increased strain levels, enhancing material flow and resulting in improved weld quality, material mixing, and desirable microstructural modifications.

References

- [1] M. Akbari, P. Asadi, T. Sadowski, "A review on friction stir welding/processing: Numerical modeling", 2023.
- [2] E.A.T. López, A.J. Ramirez, "Effect of process parameters in obtaining aluminium–steel joints and their microstructure by friction stir welding (fsw)", *Welding International*, Vol. 29, No. 9, 2015, pp. 689-697.
- [3] M. Akbari, M. Aliha, F. Berto, "Investigating the role of different components of friction stir welding tools on the generated heat and strain", *Forces in Mechanics*, Vol. 10, No. 2023, pp. 100166.
- [4] S. Singh, V.J. Badheka, V.S. Gadakh, "Assisted cooling approach for fsw of pure copper", *Welding International*, Vol. 36, No. 1, 2022, pp. 1-8.
- [5] T. Ghidini, T. Vugrin, C. Dalle Donne, "Residual stresses, defects and non-destructive evaluation of fsw joints", *Welding International*, Vol. 19, No. 10, 2005, pp. 783-790.
- [6] X. Lu, J. Qiao, J. Qian, S. Sun, S.Y. Liang, "Welding parameters optimization during plunging and dwelling phase of fsw 2219 aluminum alloy thick plate", *The International Journal of Advanced Manufacturing Technology*, Vol. 120, No. 9-10, 2022, pp. 6163-6173.
- [7] X. Lu, B. Yang, Y. Zhou, S. Sun, S.Y. Liang, "Influence of process parameters on temperature field, microstructure, and mechanical properties of fsw thick aluminum alloy 2219", *J. of Materi Eng and Perform*, Vol. No. 2023, pp. 1-11.
- [8] G. Ma, H. Gao, C. Sun, Y. Gu, J. Zhao, Z. Fang, "Probing the anti-corrosion behavior of x65 steel underwater fsw joint in simulated seawater", *Frontiers in Materials*, Vol. 8, No. 2022, pp. 723986.

- [9] M. Khedr, A. Hamada, A. Järvenpää, S. Elkatatny, W. Abd-Elaziem, "Review on the solid-state welding of steels: Diffusion bonding and friction stir welding processes", *Metals*, Vol. 13, No. 1, 2022, pp. 54.
- [10] M. Regev, B. Almoznino, S. Spigarelli, "A study of the metallurgical and mechanical properties of friction-stir-welded pure titanium", *Metals*, Vol. 13, No. 3, 2023, pp. 524.
- [11] N. Raut, V. Yakkundi, V. Sunnapwar, T. Medhi, V.K.S. Jain, "A specific analytical study of friction stir welded ti-6al-4v grade 5 alloy: Stir zone microstructure and mechanical properties", *Journal of Manufacturing Processes*, Vol. 76, No. 2022, pp. 611-623.
- [12] V. Lunetto, M. De Maddis, P. Russo Spena, "Similar and dissimilar lap friction stir welding of titanium alloys: On the elimination of the hook defect", *The International Journal of Advanced Manufacturing Technology*, Vol. 126, No. 7-8, 2023, pp. 3417-3435.
- [13] M. Akbari, H. Rahimi Asiabarak, "Modeling and optimization of tool parameters in friction stir lap joining of aluminum using rsm and nsga ii", *Welding International*, Vol. 37, No. 1, 2023, pp. 21-33.
- [14] M. Akbari, H. Rahimi Asiabarak, E. Hassanzadeh, M. Esfandiari, "Simulation of dissimilar friction stir welding of aa7075 and aa5083 aluminium alloys using coupled eulerian-lagrangian approach", *Welding International*, Vol. 37, No. 4, 2023, pp. 174-184.
- [15] K. Fuse, V. Badheka, "Bobbin tool friction stir welding: A review", *Science and Technology of Welding and Joining*, Vol. 24, No. 4, 2019, pp. 277-304.
- [16] M.M. Ahmed, K. Touileb, M.M. El-Sayed Seleman, I. Albaijan, M.I. Habba, "Bobbin tool friction stir welding of aluminum: Parameters optimization using taguchi experimental design", *Materials*, Vol. 15, No. 8, 2022, pp. 2771.
- [17] M. Pecanac, D.L. Zlatanovic, N. Kulundzic, M. Dramicanin, Z. Lanc, M. Hadzistević, S. Radisic, S. Balos, "Influence of tool and welding parameters on the risk of wormhole defect in aluminum magnesium alloy welded by bobbin tool fsw", *Metals*, Vol. 12, No. 6, 2022, pp. 969.
- [18] J. Feng, Y. Li, W. Gong, D. Sun, "The microstructures and mechanical properties of underwater bobbin tool friction stir-welded 6082-t6 aluminum alloy", *The International Journal of Advanced Manufacturing Technology*, Vol. 121, No. 1-2, 2022, pp. 1443-1453.
- [19] P. Asadi, M. Mirzaei, M. Akbari, "Modeling of pin shape effects in bobbin tool fsw", *International Journal of Lightweight Materials and Manufacture*, Vol. 5, No. 2, 2022, pp. 162-177.
- [20] Y. Sun, W. Liu, Y. Li, S. Sun, W. Gong, "Study on temperature field, microstructure, and properties of t2 pure copper by bobbin tool friction stir welding", *The International Journal of Advanced Manufacturing Technology*, Vol. 127, No. 3, 2023, pp. 1341-1353.
- [21] G.-Q. Wang, Y.-H. Zhao, Y.-Y. Tang, "Research progress of bobbin tool friction stir welding of aluminum alloys: A review", *Acta Metallurgica Sinica (English Letters)*, Vol. 33, No. 1, 2020, pp. 13-29.
- [22] M. Esmaily, A. Mortazavi, W. Osikowicz, H. Hindsefelt, J.-E. Svensson, M. Halvarsson, J. Martin, L.-G. Johansson, "Bobbin and conventional friction stir welding of thick extruded aa6005-t6 profiles", *Materials & Design*, Vol. 108, No. 2016, pp.
- [23] K. Fuse, V. Badheka, A.D. Oza, C. Prakash, D. Buddhi, S. Dixit, N.I. Vatin, "Microstructure and mechanical properties analysis of al/cu dissimilar alloys joining by using conventional and bobbin tool friction stir welding", 2022.
- [24] D. Sejani, W. Li, V. Patel, "Stationary shoulder friction stir welding—low heat input joining technique: A review in comparison with conventional fsw and bobbin tool fsw", *Critical Reviews in Solid State and Materials Sciences*, Vol. 47, No. 6, 2022, pp. 865-914.
- [25] K. Fuse, V. Badheka, A.D. Oza, C. Prakash, D. Buddhi, S. Dixit, N. Vatin, "Microstructure and mechanical properties analysis of al/cu dissimilar alloys joining by using conventional and bobbin tool friction stir welding", *Materials*, Vol. 15, No. 15, 2022, pp. 5159.
- [26] P. Asadi, R.A. Mahdavejad, S. Tutunchilar, "Simulation and experimental investigation of fsp of az91 magnesium alloy", *Materials Science and Engineering: A*, Vol. 528, No. 21, 2011, pp. 6469-6477.
- [27] G. Buffa, A. Ducato, L. Fratini, "Fem based prediction of phase transformations during friction stir welding of ti6al4v titanium alloy", *Materials Science and Engineering: A*, Vol. 581, No. 0, 2013, pp. 56-65.
- [28] B. Meyghani, M. Awang, "The influence of the tool tilt angle on the heat generation and the material behavior in friction stir welding (fsw)", *Metals*, Vol. 12, No. 11, 2022, pp. 1837.
- [29] O.S. Salih, H. Ou, W. Sun, "Heat generation, plastic deformation and residual stresses in friction stir welding of aluminium alloy", *International Journal of Mechanical Sciences*, Vol. 238, No. 2023, pp. 107827.
- [30] M. Esmaily, N. Mortazavi, W. Osikowicz, H. Hindsefelt, J.E. Svensson, M. Halvarsson, J. Martin, L.G. Johansson, "Bobbin and conventional friction stir welding of thick extruded aa6005-t6 profiles", *Materials & Design*, Vol. 108, No. 2016, pp. 114-125.

- [31] M. Mirzaei, P. Asadi, A. Fazli, "Effect of tool pin profile on material flow in double shoulder friction stir welding of az91 magnesium alloy", *International Journal of Mechanical Sciences*, Vol. 183, No. 2020, pp. 105775.
- [32] J.-y. LI, X.-p. ZHOU, C.-l. DONG, J.-h. DONG, "Temperature fields in 6082 aluminum alloy samples bobbin-tool friction stir welded", *Journal of Aeronautical Materials*, Vol. 33, No. 5, 2013, pp. 36-40.
- [33] M. Akbari, M. Aliha, S. Keshavarz, A. Bonyadi, "Effect of tool parameters on mechanical properties, temperature, and force generation during fsw", *Proceedings of the Institution of Mechanical Engineers, Part L: Journal of Materials: Design and Applications*, Vol. 233, No. 6, 2019, pp. 1033-1043.
- [34] D. Hattingh, T. Van Niekerk, C. Blignault, G. Kruger, M. James, "Analysis of the fsw force footprint and its relationship with process parameters to optimise weld performance and tool design", *Weld World*, Vol. 48, No. 2004, pp. 50-58.
- [35] C. Chen, R. Kovacevic, "Thermomechanical modelling and force analysis of friction stir welding by the finite element method", *Proceedings of the Institution of Mechanical Engineers, Part C: Journal of Mechanical Engineering Science*, Vol. 218, No. 5, 2004, pp. 509-519.
- [36] M.S. Jaffarullah, C.Y. Low, M.S.B. Shaari, A. Jaffar, "A review of force control techniques in friction stir process", *Procedia Computer Science*, Vol. 76, No. 2015, pp. 528-533.
- [37] M. Akbari, P. Asadi, T. Sadowski, "A review on friction stir welding/processing: Numerical modeling", *Materials*, Vol. 16, No. 17, 2023, pp. 5890.
- [38] M. Akbari, M.R.M. Aliha, S.M.E. Keshavarz, A. Bonyadi, "Effect of tool parameters on mechanical properties, temperature, and force generation during fsw", *Proceedings of the Institution of Mechanical Engineers, Part L: Journal of Materials: Design and Applications*, Vol. 233, No. 6, 2016, pp. 1033-1043.
- [39] F.F. Wang, W.Y. Li, J. Shen, Q. Wen, J.F. dos Santos, "Improving weld formability by a novel dual-rotation bobbin tool friction stir welding", *Journal of Materials Science & Technology*, Vol. 34, No. 1, 2018, pp. 135-139.
- [40] M. Akbari, P. Asadi, "Effects of different cooling conditions on friction stir processing of a356 alloy: Numerical modeling and experiment", *Proceedings of the Institution of Mechanical Engineers, Part C: Journal of Mechanical Engineering Science*, Vol. 236, No. 8, 2021, pp. 4133-4146.
- [41] D. Li, X. Yang, L. Cui, F. He, H. Shen, "Effect of welding parameters on microstructure and mechanical properties of aa6061-t6 butt welded joints by stationary shoulder friction stir welding", *Materials & Design*, Vol. 64, No. 2014, pp. 251-260.
- [42] F. Wang, W. Li, J. Shen, Z. Zhang, J. Li, J. Dos Santos, "Global and local mechanical properties and microstructure of bobbin tool friction-stir-welded al-li alloy", *Science and Technology of Welding and Joining*, Vol. 21, No. 6, 2016, pp. 479-483.